Modeling and Integration of Flexible Demand in Heat and Electricity Integrated Energy System

Changzheng Shao, *Student Member, IEEE* ,Yi Ding, *Member, IEEE,* Jianhui Wang, *Senior Member, IEEE* and Yonghua Song, *Fellow, IEEE*

***Abstract*— This paper is focused on utilizing customers' flexible energy demand, including both heat demand and electricity demand, to provide balancing resources and relieve the difficulties of integrating variable wind power with the combined heat and power (CHP). The integration of heat and electricity energy systems providing customers with multiple options for fulfilling their energy demand is described. Customer aggregators are introduced to supply downstream demand in the most economical way. Controlling customers' energy consumption behaviors enables aggregators to adjust their energy demand in response to supply conditions. Incorporating aggregators' flexible energy demand into the centralized energy dispatch model, a two-level optimization problem (TLOP) is firstly formed where the system operator maximizes social welfare subject to aggregators' strategies which minimize the energy purchase cost. Furthermore, the sub-problems are linearized based on several reasonable assumptions. Optimal conditions of the sub-problems are then transformed as energy demands to be described as explicit piecewise-linear functions of electricity prices corresponding to the demand bid curves. In this way, the TLOP is transformed to a standard optimization problem, which requires aggregators to only submit a demand bid to run the centralized energy dispatch program. All the parameters pertaining to the aggregators' energy consumption models are internalized in the bid curves. The proposed technique is illustrated in a modified testing system.**

***Index Terms*—Combined heat and power (CHP), flexible demand, linearization, integrated energy dispatch.**

NOMENCLATURE

gi, gj, gk	Index of generating units (subscript)
j	Index of customers (subscript)
i	Index of aggregators (subscript)
n, p	Index of buses (subscript)
t	Index of time intervals (superscript)
C_w	Specific heat of water ($J/(kg\,^oC)$)
T_s / T_r	Supply/return temperature (^oC)
T_a / T_n	Ambient/indoor temperature (^oC)
T_{in} / T_{out}	Inlet/outlet temperature (^oC)
m_i	Heat water mass flow (kg / s)
H	Volumetric heat index ($W/(\mathrm{m}^3\,^oC)$)
V	Peripheral volume (m^3)
l	Length of the pipe (m)
h	Heat transfer coefficient ($W/(\mathrm{m}\ ^oC)$)
R	Relative water flow ratio
η_{es}	Efficiency of electric heating
ρ	Water density (kg/m^3)
Ngj	Number of CHP units
Ngi	Number of electricity-only units
Na	Number of aggregators
NT	Number of time intervals
B_i	Benefit function of aggregator i
$G_{e,gi}$	Output of thermal electricity-only units (MW)
$G_{e,gj}$	Power output of CHP units (MW)
$G_{h,gj}$	Heat output of CHP units (MW)
Υ_{eh}	Heat-to-electricity ratio of CHP units
L_e	Total electricity demand (MW)
L_{es}	Electricity demand (heating) (MW)
L_{e0}	Electricity demand (non-heating) (MW)
$L_{h0,j}$	Heating demand of customer j (MW)
$L_{h,i}$	Heat demand of aggregator i (MW)
G_{np}	Conductance of the transmission line
B_{np}	Susceptance of the transmission line
δ	Phase angle
V	Magnitude of the bus voltage
$T^{\max}$	Transmission line capacity (MW)
η	Efficiency of electric heating
p_e , p_h	Electricity price, heat price ($/MWh)
λ	Dual variables of the constraints

I. INTRODUCTION

THE growing awareness of climate change and environmental issues entails the transition towards a low-carbon and sustainable energy system [1]. As an efficient measure to improve energy efficiency, the integrated energy systems (IES) have gained rapid development in recent years. The heat and power integrated energy system (HE-IES), based on combined heat and power (CHP), is one of the most important forms of IES [2]. Countries around the world have made great efforts to develop CHP. In Denmark, CHP covers about 40% of the demand for space heating [3]. In northern China, CHP based

Manuscript received January 17, 2017; revised May 17, 2017; accepted July 05, 2017.The research is supported by the China NSFC under Grant 51577167 and the U.S. Department of Energy (DOE)'s Office of Electricity De-livery and Energy Reliability under contract DE-OE0000839. Paper no. TSTE-00082-2017.R1. (*Corresponding author: Yi Ding*)

C. S., Y. D. and Y. S. are with the College of Electrical Engineering, Zhejiang University, Hangzhou ,310058, China (e-mail: shao-changzheng@zju.edu.cn , yiding@zju.edu.cn , yonghua-song@zju.edu.cn). J. W is with the Department of Electrical Engineering at Southern Methodist University, Dallas, TX, USA and the Energy Systems Division at Argonne National Laboratory, Argonne, IL, USA (email: jianhui.wang@ieee.org).

district heating (DH) has been installed in more than 300 cities, serving 40% of China's population [4].

However, the inharmony between the high-penetration wind power and the wide use of CHP has become a challenge for operating the energy systems [5]. On the one hand, the fluctuation of wind power makes electricity price vary significantly during the operating day. Thus, the profit of CHP units can be dramatically reduced in periods of low electricity price resulting from large wind power production [6]. On the other hand, the electricity generation of CHP units is constrained by their heat production, which must target on customers' heat demand. This leads to high wind power curtailment when the electricity production of CHP units covers most of the electricity demand during the off-peak hours[4].

Facing the challenges of integrating wind power with CHP units, a lot of researches have been conducted on increasing the flexibility of CHP based energy system. These works are mostly focused on decoupling the heat production from electricity generation by coupling CHP units with thermal storage or electric heating systems (EHS), such as heat pumps and electric boilers [7, 8]. However, these measures are more appropriate for relatively small CHP units used for district heating. For the centralized and high-capacity CHP units, it would be difficult to install the thermal stores of corresponding capacity. Moreover, the utilization of the heat storage capacity of the district heating network for increasing the flexibility has been proposed in [9].

Besides the measures from the production and network sides, the demand-side resources hold untapped potential for increasing the operational flexibility of CHP based IES. Given that the operation of CHP units is usually constrained by their heat output, encouraging customers to adjust their energy demand, especially the heat demand, in response to the supply conditions is crucial for increasing the flexibility of the energy system. Moreover, it has become a realistic possibility since more and more heating systems are transformed from constant flow systems to variable flow systems [10].

Indeed, the integration of multiple energy systems imparts flexibility to customers' energy demand. In the integrated energy system, customers have multiple options to fulfill their energy demand [11, 12]. For instance, their heating demand can be supplied through the heat power from the heat networks or the electric heating devices. Since alternate cost pricing is a common practice pricing mechanism used in DH system and electric heat pumps have come to be a price competitive alternative[13], it would be economically feasible for customers to switch to electric heating during low-electricity-price periods. Such built-in flexibility enables customers to adjust their energy demand in response to the supply conditions to reduce their energy bills. In this way, the independent system operator (ISO) will also obtain more balancing resources for maintaining the energy balance and improving the operation flexibility of the energy system. For example, when the electricity is oversupplied due to the increased electricity production from the wind power, the electricity price can be relatively low and customers therefore may increases the use of electric heating. Then, the aggregated demand for electricity increases while the demand for heat decreases. CHP units therefore can decrease the amount of heat and electricity produced. In this way, the rebalance is achieved without the curtailment of wind power and customers also benefit financially.

The potential for flexible multiple energy systems to provide demand response (DR) have been illustrated in [14-16]. These studies are more focused on identifying and quantifying their electricity shifting potential to participate in real-time DR programs. Moreover, the utilization of the demand response for releasing the heat production constraints in the HE-IES has not been discussed yet.

This paper investigates the utilization of customers' flexible energy demand, including both heat demand and electricity demand, to provide additional balancing resources for maintaining the energy supply and demand balance and avoiding the wind power curtailment. Customer aggregators are introduced to purchase energy from the centralized energy systems for supplying customer's energy demand in the most cost-effective way. Meanwhile, by controlling customers' energy consumption behaviors, aggregators are able to adjust their energy demand in response to supply conditions.

It is assumed that both electricity energy system and heat energy system are managed by a single ISO and all the aggregators seek to minimize their energy costs. Incorporating the aggregators' flexible energy demand into the central energy dispatch model therefore forms a two-level optimization problem (TLOP), where the ISO maximizes social welfare subject to aggregators' strategies in which aggregators adjust their energy demand so as to minimize the energy purchase cost. Moreover, the low-level problems are linearized based on several reasonable assumptions. KKT conditions of the low-level problems are then transformed into energy demand as explicit and piecewise-linear functions of electricity prices corresponding to the demand bid curves. In this way, it requires each aggregator to submit only a demand bid to run the centralized energy dispatch. All other parameters pertaining to the energy consumption models are internalized in the bid curves. After that, the TLOP problem is transformed into an extended optimal power flow (OPF) problem, in which electricity energy and heat energy are jointly optimized.

The proposed technique is used in a modified testing system. We find that the customers' flexible energy demand can serve as a tool to further bridge the heat and electricity energy systems from the consumption side which enables the co-optimization of the two kinds of energy systems. The illustrative results demonstrate that not only the volatility of electricity price and wind power curtailment can be reduced, but also the social welfare can be increased remarkably.

The remainder of the paper is organized as follows. Section II describes the structure and aggregator model of the HE-IES. The TLOP for joint heat and electricity dispatch is formulated in Section III. Section IV simplifies the sub-problems. The manifold benefits of the proposed technique are illustrated by the case study in Sections V. Section VI is the summary of the paper.

This article has been accepted for publication in a future issue of this journal, but has not been fully edited. Content may change prior to final publication. Citation information: DOI 10.1109/TSTE.2017.2731786, IEEE Transactions on Sustainable Energy

II. Heat and Electricity Integrated Energy System

A. Description of the HE-IES

The proposed HE-IES is a combination of CHP based heating system and electric power system, which supplies heat and electricity for customers.

The schematic graph of the HE-IES is shown in Fig.1.

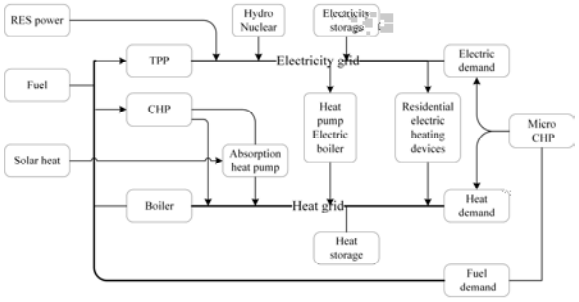

Fig. 1. Schematic graph of the HE-IES.

The system involves heat and electricity generating units, heat and electricity grids, and customers' energy demand as shown in Fig. 1.

Generally, the generating units in the HE-IES can be divided into electricity-only units, cogenerating units and heat-only units. The electricity-only units include conventional electricity generating units, such as thermal power generating units (TPP), and renewable energy power generating units (RES power, such as wind power). The cogeneration units are CHP units, and the heat-only units usually refer to boilers. Moreover, the heat and electricity production of a CHP unit are coupled, which have to stay within the feasible operating area [7].

The heat produced by the CHP units is delivered to the customers through the DH networks, to which the CHP units and customers' buildings are connected. After generation, the heat is distributed to the customers via the DH network of pipes. At customer level the heat network is usually connected to the central heating system of the dwellings via substations[17]. In a DH system intended to supply a customers' energy requirement, two parameters can be controlled: supply temperature and flow rate[18].Moreover, more and more DH networks are transformed to variable flow systems, which allows the heat output to change when some of the customers' heating demand changes. It is suggested that modern DH schemes give customers just as much control as individual gas boilers and could be very efficient[17].

B. Modelling the Customer Aggregators' Energy Demand

Customer aggregators as an independent entity is in charge of purchasing energy from the energy market and supplying the downstream demands. The aggregator can be modelled as a heat and electricity integrated energy consumption node, as shown in Fig.2.

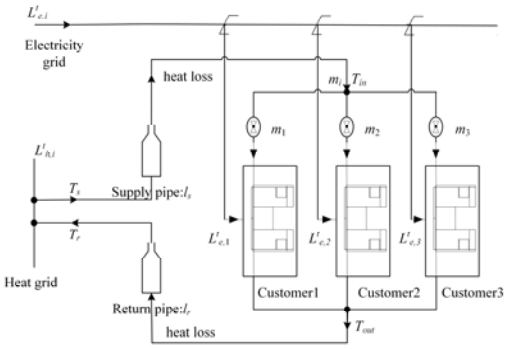

Fig. 2. Schematic diagram of the aggregator' energy demand.

1) Energy Demand of the Aggregator

Energy demand of the aggregator is defined as the demand for the imported electricity and heat from the energy grids. The electricity demand of the aggregator is equal to the sum of the electricity demand of all the customers, which is expressed as:

$$L_{e,i} = \sum_{j \in \Xi_i} L_{e,j} \tag{1}$$

where Ξ_i identifies the set of customers served by the aggregator i .

The heat demand of the aggregator can be calculated as:

$$L_{h,i} = m_i C_w (T_s - T_r) \tag{2}$$

2) Heating Network

A heat source supplies heat by means of hot water or steam, and then the heat power is delivered to the customers through the heating network. A heating network consists of supply pipes and return pipes. Heating systems can be controlled with constant flow and constant temperature, constant flow and variable temperature, variable flow and constant temperature, or variable flow and variable temperature[17]. Moreover, more district heating systems are transformed from constant flow systems to variable flow system [19]. In this paper, it is assumed that the heating systems are operated with variable flow and constant temperature, i.e. T_s is maintained constant and m_i may vary within the selected range.

The temperature drops exponentially during water flow in pipes[20], hence:

$$\begin{aligned} T_{in} &= (T_s - T_a) e^{-hl_s / c_w m_i} + T_a \\ T_{out} &= (T_r - T_a) e^{hl_r / c_w m_i} + T_a \end{aligned} \tag{3}$$

where l_s and l_r are the length of the supply pipe and return pipe, respectively. Usually, it can be assumed that $l_s = l_r = l$.

Moreover, as we can see from Fig.2, the heat loss in the network can be expressed as:

$$P_h^{loss} = C_w m_i (T_s - T_r) - C_w m_i (T_{in} - T_{out}) \tag{4}$$

As shown in (3) and (4), the heat loss is related to the gross water flow (which is dependent on the heating demand), ambient temperature, the length of the heat pipe, and so on.

The gross water flow of the heating system equals to the sum of the flow of the pumps at customer sites, which is expressed as:

$$m_i = \sum_{j \in \Xi_i} m_j \tag{5}$$

Moreover, it is defined that: $m_j = R_j m_j^{set}$, where m_j^{set} is the rated water flow, and R_j is the relative water flow ratio.

3) Electricity Power Balance

The electricity demand of the customer j can be divided to heating-demand $L_{es,j}$ and non-heating demand $L_{e0,j}$. The non-heating demand includes the lighting, pumps, fans and other electric appliances. The electricity demand $L_{e,j}$ is the sum of the heating-demand and non-heating demand, which is expressed as:

$$L_{e,j} = L_{es,j} + L_{e0,j} \tag{6}$$

4) Heat Power Balance

There is a direct relationship between heating load and the temperature difference between the inside and outside of the customers' building. The more the temperature difference is, the more the heating demand is. Generally, indoor temperature of customer j is centrally controlled and is assumed to be the same as that of other customers. The heating load of customer j is estimated as:

$$L_{h0,j} = H_j V_j (T_n - T_a) \tag{7}$$

The heat supplied to customer j comes from heating radiators and electric heating devices. The total value of heat injected into the customer's building $H_{in,j}$ can be calculated as the following:

$$H_{in,j} = H_{es,j} + H_{net,j} = \eta_j L_{es,j} + m_j C_w (T_{in} - T_{out}) \tag{8}$$

where $H_{es,j}$ and $H_{net,j}$ are the heat release rate of the electric heating device and the radiator installed for customer j, respectively. $L_{es,j}$ is the electric power input of the electric heating and η_j represents its efficiency.

Therefore, the response of the indoor temperature of customer j can be expressed as:

$$\rho_j C_w V_j \frac{dT_n}{dt} = \eta_j L_{es,j} + m_j C_w (T_{in} - T_{out}) - L_{h0,j} \tag{9}$$

III. TLOP-Formulation of the Dispatch Model

In this paper, it is assumed that both the electricity system and heat system are managed by a single ISO. The ISO runs a centralized energy dispatch model for the dispatch of heat energy and electricity energy. As aforementioned, the integration of heat energy and electricity energy imparts flexibility to customer's energy demand. The flexibility can be further managed and aggregated by the aggregators. Moreover, the energy market is able to provide economic incentives to offer flexibility through real-time price mechanism. Aggregators in charge of controlling customer's energy consumption pattern could take advantage of these incentives for minimizing the energy purchase cost. The aggregators' response, in return, provides additional flexibility to power system operators, which is necessary to the transition towards more renewable generation.

However, it should be noted that the aggregators' adjusting their energy demand introduces additional uncertainty to the energy system operation. Usually, it can be assumed that all aggregators are rational market participants who try to minimize the energy purchase cost. As a result, the centralized dispatch model forms a two-level optimization problem where the ISO maximizes the social welfare based on all bids in the market subject to a sub solution where the aggregators minimize the energy purchase cost based on the energy prices. To be specific, aggregators are supposed to send information on their energy consumption models to the ISO in the proposed approach. The ISO runs the centralized energy dispatch model with the consideration of the aggregators' optimal strategy. In this way, the clearing results guarantee not only the optimal solution for the total energy system, but also the minimum costs for all aggregators. Hence, the convergence to an equilibrium among all aggregators can be guaranteed.

The formulation of the two-level optimization is shown in (10)-(29).

$$\underset{G_{e,gi}^t, G_{e,gj}^t, G_{h,gj}^t}{Maximize}\ F = \sum_{t=1}^{NT} \Big(\sum_{i=1}^{Na} B_i (L_{e,i}^t, L_{h,i}^t) - \sum_{gi=1}^{Ngi} C_{gi}^t (G_{e,gi}^t) - \sum_{gj=1}^{Ngj} C_{gj}^t (G_{e,gj}^t, G_{h,gj}^t) \Big) \tag{10}$$

Subject to:

$$\sum_{gi \in \Psi_n} G_{e,gi}^t + \sum_{gj \in \Psi_n} G_{e,gj}^t - \sum_{i \in \Psi_n} L_{e,i}^t = \sum_{p \in \Theta_n} V_n V_p \left[G_{np} \cos(\delta_n^t - \delta_p^t) + B_{np} \sin(\delta_n^t - \delta_p^t) \right] \tag{11}$$

$$\sum_{n \in \Pi_d} \sum_{gj \in \Psi_n} G_{h,gj}^t = \sum_{n \in \Pi_d} \sum_{i \in \Psi_n} L_{h,i}^t \quad \forall t \tag{12}$$

$$\underline{G_{e,gi}^t} \le G_{e,gi}^t \le \overline{G_{e,gi}^t} \quad \forall t, \forall gi \tag{13}$$

$$\underline{G_{e,gj}^t} \le G_{e,gj}^t \le \overline{G_{e,gj}^t} \quad \forall t, \forall gj \tag{14}$$

$$\underline{G_{h,gj}^t} \le G_{h,gj}^t \le \overline{G_{h,gj}^t} \quad \forall t, \forall gj \tag{15}$$

$$G_{h,gj}^t = \Upsilon_{he,gj} G_{e,gj}^t \tag{16}$$

$$-T_{np}^{\max} \le T_{np} \le T_{np}^{\max}, \ \forall p \in \Theta_n \tag{17}$$

$$-\pi \le \delta_n^t \le \pi \quad \forall t, \forall n \tag{18}$$

$$(L_{e,i}^t, L_{h,i}^t) \in \arg\ \text{minimize}\ p_e^t L_{e,i}^t + p_h L_{h,i}^t \tag{19}$$

subject to:

$$L_{e,i}^t = \sum_{j \in \Xi_i} L_{e,j}^t \tag{20}$$

$$L_{h,i}^t = m_i^t C_w (\mathrm{T}_s - \mathrm{T}_r) \tag{21}$$

$$m_i^t = \sum_{j \in \Xi_i} m_j^t \tag{22}$$

$$m_j^t = R_j^t m_j^{set}, \quad \forall t, \forall j \tag{23}$$

$$\eta_j L_{es,j}^t + m_j^t C_w (T_{in}^t - T_{out}^t) - L_{h0,j}^t = 0 \ \forall t, \forall j \tag{24}$$

$$T_{in}^t = (T_s - T_a^t) e^{hl / c_w m_i^t} + T_a^t \tag{25}$$

$$T_{out}^t = (T_r - T_a^t) e^{hl / c_w m_i^t} + T_a^t \tag{26}$$

$$L_{e,j}^t = L_{es,j}^t + L_{e0,j}^t \quad \forall j \in \Xi_i \tag{27}$$

$$\underline{R} \le R_j^t \le \overline{R} \quad \forall t, \forall j \tag{28}$$

$$p_e^t = \lambda_n^t \tag{29}$$

The high-level problem (10)–(18) represents the centralized energy dispatch with the target of maximizing the social welfare. Equation (11) and (12) represent the power balance and heat balance, respectively. Since this paper is focused on the steady state, the heating network in a heating district is equivalent to a single node, where only the heat balance is considered, as shown in (12) [21]. Equations (13)–(15) are power output bounds for the generating units. Constraints (17) enforces the transmission capacity limits of each line. Constraints (18) stands for angle bounds for each node. $n \in \Pi_d$ identifies the node belongs to heating district d. $gi \in \Psi_n$ identifies the thermal power generating unit located at bus n. $p \in \Theta_n$ identifies the bus p connected to bus n. $\Upsilon_{he,gj}$ is the heat-to-electricity ratio of the *gj*-th CHP unit. It should be noted that the heat demand and electricity demand ($L^t_{e,i}$, $L^t_{h,i}$) are endogenously generated within the lower-level problem.

The low-level problem (19)–(29) represents strategy of aggregator i for minimizing the energy purchase cost. Equation (24) enforces a constant indoor temperature of customers' building to ensure comfort. λ_n^t is the dual variable on the equilibrium constraint, obtained from the high-level problem.

The most common approach to solving the TLOP is to replace the sub-problems by their KKT conditions [22]. In this way, the TLOP can be written as a standard optimization problem. However, it requires the detailed parameters pertaining to aggregators' energy consumption model when ISO runs the centralized energy dispatch program, as can be seen from its formulation. Considering that the aggregators can be in large number and widely distributed, it would be impractical for aggregators to send detailed energy consumption models to the ISO. Moreover, considering all the parameters is bound to increase the computation burden, it is necessary to modify the TLOP by simplifying the KKT conditions of the low-level problems.

IV. Simplifying the Sub-problems' KKT conditions

As discussed above, a TLOP is presented in which aggregators try to minimize their energy purchase cost under the constraint that their dispatch and price are determined by the centralized energy dispatch. Usually, the TLOP can be solved by representing the sub-problems with the KKT conditions. This paper try to linearize the sub-problems by linearizing the nonlinear constraints. After that, the KKT conditions of the sub-problems can be represented by a set of linear constraints, which are modelled as the energy demands as explicit linear functions of electricity price corresponding to the demand bid curves. In this way, the TLOP is transformed to a standard optimization problem, which requires aggregators to only submit a demand bid to run the centralized energy dispatch program.

In this section, reasonable assumptions are made for the simplification of the low-level problems. More specifically, the inequality constrains are linearized, making it possible to find the linear relationships between the energy demand $L^t_{e,i}, L^t_{h,i}$ and electricity price in the KKT conditions.

As aforementioned, the temperature distribution along the heating pipes can be expressed as:

$$\begin{aligned} T_{in} &= (T_s - T_a)e^{-hl/c_w m} + T_a \\ T_{out} &= (T_r - T_a)e^{hl/c_w m} + T_a \end{aligned} \tag{3}$$

In practice, $\mu = hl_r / c_w m_i^t$ is very small. Using the equivalent infinitesimal $\lim_{\mu \to 0} e^{\mu} = 1 + \mu$, (3) can be approximately written as[20]:

$$\begin{aligned} T^t_{in} &= (T_s - T^t_a)(1 - hl / c_w m^t_i) + T^t_a \\ T^t_{out} &= (T_r - T^t_a)(1 + hl / c_w m^t_i) + T^t_a \end{aligned} \tag{30}$$

Moreover, it is reasonable to assume that the rated water flow is determined by and proportional to the customers' heating load, that is:

$$m^{set}_j \Big/ \sum_{j \in \Xi_i} m^{set}_j = L^t_{h0,j} \Big/ \sum_{j \in \Xi_i} L^t_{h0,j} = K_j \tag{31}$$

Following this assumption, the heat power balance constraint (24) can be expressed as

$$\eta_j L^t_{es,j} + C_w \left[(T_s - T_r) m^t_j - \frac{m^t_j}{m^t_i} (T_s + T_r - 2T_a^t) \frac{hl}{C_w} \right] = L_{h0,j} \tag{32}$$

Moreover, m_i^t is approximated as:

$$m^t_i = \sum_{j \in \Xi_i} m^t_j = \sum_{j \in \Xi_i} R^t_j m^t_j \approx R_{av} \sum_{j \in \Xi_i} m^{set}_j \tag{33}$$

where $R_{av} = \left(\underline{R} + \overline{R} \right) \Big/ 2$.

Hence, (24) (25) and (26) are replaced by:

$$\eta_j L^t_{es,j} + C_w \left[(T_s - T_r) m^{set}_j - \frac{K_j}{R_{av}} (T_s + T_r - 2T_a^t) \frac{hl}{C_w} \right] R^t_j = L_{h0,j} \tag{34}$$

Since the nonlinear constraints in the low-level problem is linearized, the low-level problem is transformed to a linear optimization problem. The KKT conditions of the low-level problems therefore can be transformed to heat demand and electricity demand as explicit piecewise-linear functions of electricity price.

To facilitate the understanding of the simplified optimal conditions, a case is illustrated where $j = \{1,2,3\}$. The optimal strategy of the aggregator can be described as:

$$\begin{aligned} \underset{L^t_{ei}, L^t_{h,i}, L^t_{es,j}, R^t_j}{\text{minimize}} \quad & p^t_e L^t_{e,i} + p_h L^t_{h,i} \\ s.t. \quad & L^t_{e,i} = \textstyle\sum_{j=1,2,3} (L^t_{es,j} + L^t_{e0,j}) \\ & L^t_{h,i} = \textstyle\sum_{j=1,2,3} R^t_j m^{set}_j C_w (\mathrm{T}_s - \mathrm{T}_r) \\ & \eta_j L^t_{es,j} + \zeta^t_j R^t_j - L^t_{h0,j} = 0 \quad \forall t, \forall j = 1,2,3 \\ & \underline{R} \le R^t_j \le \overline{R} \quad \forall t, \forall j = 1,2,3 \end{aligned} \tag{35}$$

where $\zeta^t_j = \left[(T_s - T_r) C_w m^{set}_j - \frac{K_j}{R_{av}} (T_s + T_r - 2T_a^t) hl \right]$

The Lagrange function of the optimization problem is expressed as:

This article has been accepted for publication in a future issue of this journal, but has not been fully edited. Content may change prior to final publication. Citation information: DOI 10.1109/TSTE.2017.2731786, IEEE Transactions on Sustainable Energy

$$\begin{aligned} L = {} & p_e^t L_{e,i}^t + p_h L_{h,i}^t + \lambda_e (L_{e,i}^t - \sum\nolimits_{j=1,2,3} (L_{es,j}^t + L_{e0,j}^t)) \\ & + \lambda_h (L_{h,i}^t - \sum\nolimits_{j\in \Xi_i} R_j^t m_j^{set} C_w (\mathrm{T}_s - \mathrm{T}_r)) \\ & + \sum\nolimits_{j=1,2,3} (\lambda_{eh,j} (\eta_j P_{es,j}^t + \zeta_j^t R_j^t - L_{h0,j}^t)) \\ & + \sum\nolimits_{j=1,2,3} (\underline{\mu_{R,j}} (-R_j^t + \underline{R_j^t})) + \sum\nolimits_{j=1,2,3} \overline{(\mu_{R,j}} (R_j^t - \overline{R_j^t})) \end{aligned} \tag{36}$$

The KKT conditions then can be expressed as[23]:

$$\partial L / \partial L_{e,i}^t = p_e^t + \lambda_e = 0$$

$$\partial L / \partial L_{h,i}^t = p_h + \lambda_h = 0$$

for $j = 1,2,3$: (37)

$$\begin{cases} \partial L / \partial L_{es,j}^t = -\lambda_e + \lambda_{eh,j} \eta_j = 0 \\ \partial L / \partial R_j^t = -m_j^{set} C_w (\mathrm{T}_s - \mathrm{T}_r) \lambda_h + \zeta_j^t \lambda_{eh,j} - \underline{\mu_{R,j}} + \overline{\mu_{R,j}} = 0 \end{cases}$$

Define $\gamma_{eh,j} = \eta_j (T_s - T_r) C_w m_j^{set} / \zeta_j^t$, and assume $\gamma_{eh,1} > \gamma_{eh,2} > \gamma_{eh,3}$. The optimal electricity demand and heat demand of the aggregator derived from the KKT conditions are expressed in (38) and (39), respectively.

$$L_{e,i}^t = \begin{cases} L_{e0,i}^t + \underline{L_{es,1}^t} + \underline{L_{es,2}^t} + \underline{L_{es,3}^t} & : p_e^t > \gamma_{eh,1} p_h \\ L_{e0,i}^t + L_{es,1}^t (R_1^t) + \underline{L_{es,2}^t} + \underline{L_{es,3}^t} & : \underline{R} < R_1^t < \overline{R},\ p_e^t = \gamma_{eh,1} p_h \\ L_{e0,i}^t + \overline{L_{es,1}^t} + \underline{L_{es,2}^t} + \underline{L_{es,3}^t} & : \gamma_{eh,1} p_h > p_e^t > \gamma_{eh,2} p_h \\ L_{e0,i}^t + \overline{L_{es,1}^t} + L_{es,2}^t (R_2^t) + \underline{L_{es,3}^t} & : \underline{R} < R_2^t < \overline{R},\ p_e^t = \gamma_{eh,2} p_h \\ L_{e0,i}^t + \overline{L_{es,1}^t} + \overline{L_{es,2}^t} + \underline{L_{es,3}^t} & : \gamma_{eh,2} p_h > p_e^t > \gamma_{eh,3} p_h \\ L_{e0,i}^t + \overline{L_{es,1}^t} + \overline{L_{es,2}^t} + L_{es,3}^t (R_3^t) & : \underline{R} < R_3^t < \overline{R},\ p_e^t = \gamma_{eh,3} p_h \\ L_{e0,i}^t + \overline{L_{es,1}^t} + \overline{L_{es,2}^t} + \overline{L_{es,3}^t} & : p_e^t < \gamma_{eh,3} p_h \end{cases} \tag{38}$$

where $L_{e0,i}^t = L_{e0,1}^t + L_{e0,2}^t + L_{e0,3}^t$, $L_{es,j}^t (R_j^t) = (L_{h0,j}^t - \zeta_j^t R_j^t) / \eta_j$, $\underline{L_{es,j}^t} = (L_{h,j}^t - \zeta_j^t \overline{R}) / \eta_j$, $\overline{L_{es,j}^t} = (L_{h,j}^t - \zeta_j^t \underline{R}) / \eta_j$.

$$L_{h,i}^t = \begin{cases} \zeta_1^t \overline{R} + \zeta_2^t \overline{R} + \zeta_3^t \overline{R} & p_e^t > \gamma_{eh,1} p_h \\ \zeta_1^t R_1^t + \zeta_2^t \overline{R} + \zeta_3^t \overline{R} : & \underline{R} < R_1^t < \overline{R} \quad p_e^t = \gamma_{eh,1} p_h \\ \zeta_1^t \underline{R} + \zeta_2^t \overline{R} + \zeta_3^t \overline{R} : & \gamma_{eh,1} p_h > p_e^t > \gamma_{eh,2} p_h \\ \zeta_1^t \underline{R} + \zeta_2^t R_2^t + \zeta_3^t \overline{R} : & \underline{R} < R_2^t < \overline{R} \quad p_e^t = \gamma_{eh,2} p_h \\ \zeta_1^t \underline{R} + \zeta_2^t \underline{R} + \zeta_3^t \overline{R} : & \gamma_{eh,2} p_h > p_e^t > \gamma_{eh,3} p_h \\ \zeta_1^t \underline{R} + \zeta_2^t \underline{R} + \zeta_3^t R_3^t : & \underline{R} < R_3^t < \overline{R} \quad p_e^t = \gamma_{eh,3} p_h \\ \zeta_1^t \underline{R} + \zeta_2^t \underline{R} + \zeta_3^t \underline{R} : & p_e^t < \gamma_{eh,3} p_h \end{cases} \tag{39}$$

The electricity demand described in graphical mode is shown in Fig.3 where the abscissa stands for the electricity demand $L_{e,i}^t$ and the ordinate stands for electricity price p_e^t.

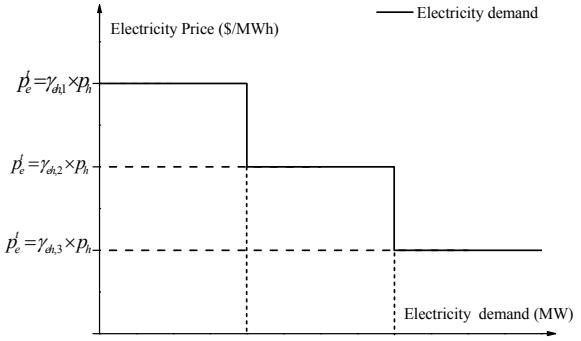

Fig. 3. Electricity demand derived from the KKT conditions

As shown in Fig.3, the electricity demand is expressed in a decreasing piecewise-linear function of the electricity price corresponding to a demand bid curve [24].

Heat demand can be expressed in a manner analogous to the electricity demand as shown in Fig.4. A heat demand function is described in Fig.4, which is mathematically similar to the electricity demand, except the demand function increases as the electricity price increases.

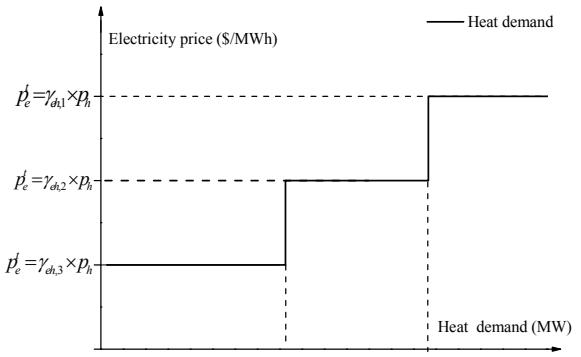

Fig. 4. Heat demand derived from the KKT conditions

In this way, KKT conditions are represented as the electricity demand and heat demand as functions of real-time electricity price. As the electricity demand and heat demand functions guarantee the optimal solution for the aggregator, the aggregator therefore can choose them as the demand bids for minimizing the energy purchase cost. Moreover, it is no longer necessary for ISO to obtain the detailed energy consumption models of aggregators, since all the parameters pertaining to energy demand and operational constraints at the customers' side are internalized in the demand bids.

The TLOP is simplified to an extended OPF problem consequently, which clears both heat and electricity and involves demand bids. The formulation can be expressed as:

$$\begin{aligned} \underset{PG_{t,gi}^t, PG_{c,gj}^t, HG_{c,gj}^t}{\text{Maxmize}} \quad & F = \sum\nolimits_{t=1}^{NT} (\sum\nolimits_{i=1}^{Na} B_i (L_{e,i}^t, L_{h,i}^t) \\ & - \sum\nolimits_{gi=1}^{Ngi} C_{gi}^t (G_{\mathrm{e},gi}^t) - \sum\nolimits_{gj=1}^{Ngj} C_{gj}^t (G_{e,gj}^t, G_{h,gj}^t)) \\ s.\mathrm{t}. \quad & (11) - (19) \\ & (38) - (39) \end{aligned} \tag{40}$$

This article has been accepted for publication in a future issue of this journal, but has not been fully edited. Content may change prior to final publication. Citation information: DOI 10.1109/TSTE.2017.2731786, IEEE Transactions on Sustainable Energy

The optimization problem is a joint heat and electricity energy dispatch model, involving many equality and inequality constraints. Among all the algorithms proposed for the solution of such an optimization problem, interior-point methods (IPMs) have shown good properties in terms of fast convergence and numeric robustness. In this paper, the optimization model is solved using a primal-dual interior point solver called MIPS, for Matlab Interior Point Solver, which is derived from the algorithms described in [25].

V. Application and Test Results

A. Test System and Scenarios

A test system is introduced to illustrate the technique proposed in this paper, in which the energy exchange happens at sub-transmission networks with voltage level in a range between 30KV and 60KV level. The system is developed from the 30-bus system [26] with six thermal power generating units (G1-G6), three wind farms (W1-W3) and three CHP units (C1-C3). The topology diagram of the electric part is shown in Fig.5.a.

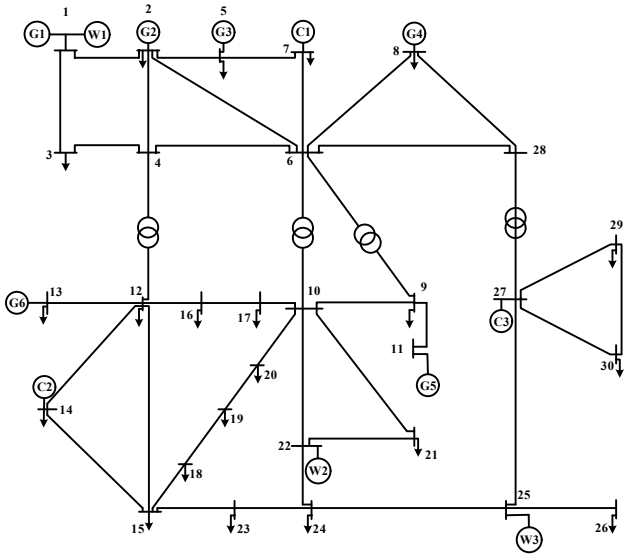

Fig. 5.a. Topology diagram of the electric power system.

Customers' maximum electricity demand can be found in [26] and it is assumed that the heat demand has the same maximum value. The capacity of each CHP unit is set as 100MW. At each node, the customers are connected to the DH network using heating substations. Moreover, the customers are aggregated and there is one aggregator for every 500-kW customers. For instance, the total heat demand at bus 26 is 3.5MW, hence, there are 7 aggregators at this bus. The topology diagram of the district heating system at bus 26 is shown in Fig.5.b.

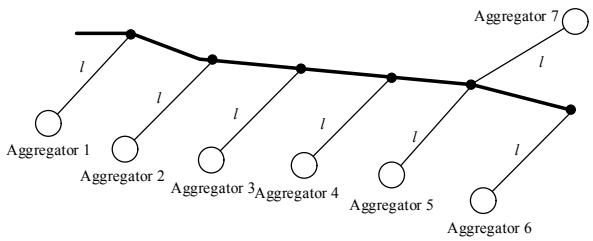

Fig. 5.b. Topology diagram of the district heating system.

The profiles of the hourly electricity demand (corresponding to $L^t_{e0,i} = \sum L^t_{e0,j}$), wind power potential, and heat demand (corresponding to $\sum L^t_{h0,j}$) are shown in Fig. 6. The electricity demand and heat demand profiles are derived from [27].

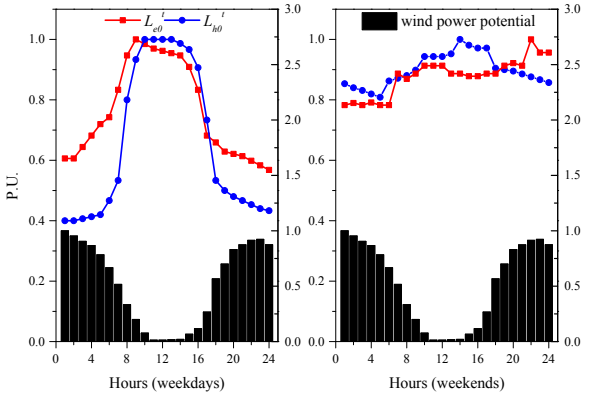

Fig. 6. Electricity and heat demand as well as wind power output.

The parameters for building the demand bids of aggregators and calculating the heat losses are shown in Table I[20].

TABLE I
Parameters of Heating Networks

Parameter	Value	Parameter	Value
C_w	4200	T_n	-9
h	0.25	$\overline{R}$	1
l	300	$\underline{R}$	0.6
T_s	85	$K_1 / K_2 / K_3$	0.2/0.3/0.5
T_r	60	$\eta_1 / \eta_2 / \eta_3$	0.8/0.85/0.9

Moreover, all the CHP units have a fixed heat-to-electricity ratio of 1.175. The economic parameters of the generating units are shown in Table II, where $a/b/c$ are the coefficients of the quadratic cost functions, i.e.

$$C^t_{gj} = a_e(G^t_{e,gj})^2 + b_e(G^t_{e,gj}) + c_e + a_h(G^t_{h,gi})^2 + b_h(G^t_{h,gi}) + c_h \quad ,$$

$$C^t_{gi} = a_e(G^t_{e,gi})^2 + b_e(G^t_{e,gi}) + c_e \quad .$$

TABLE II
Economy Parameters of Generating Units

Unit	$a_e / b_e / c_e$	$a_h / b_h / c_h$
G1	0.097/50/0	---
G2	0.097/50/0	---
G3-G6	0.03/100/0	---
C1-C3	0.015/95/0	0.015/95/0
W1-W3	0	---

To illustrate the effectiveness of the proposed technique, two scenarios (S1 and S2) are modeled: in S1, the flexibility in customers' energy demand is not considered. Compared with S1, aggregators are in charge of controlling customers' energy consumption behaviors and change their energy demand in response to the supply conditions in S2. In this scenario, aggregators submit the demand bids to the ISO to participate in the centralized energy dispatch program. In other word, the aggregators' electricity demand and heat demand in this case are elastic and price dependent.

This article has been accepted for publication in a future issue of this journal, but has not been fully edited. Content may change prior to final publication. Citation information: DOI 10.1109/TSTE.2017.2731786, IEEE Transactions on Sustainable Energy

The proposed model is applied over a 24-h horizon to the test system. Moreover, it is tested on a PC with Intel 2.4 GHz 2-core processor (4MB L3 cache), 8 GB memory. The time consumed for simulation is about 0.63s-0.74s.The simulation results from the two scenarios are analyzed in terms of electricity price volatility, wind power accommodation and social welfare.

B. Simulation Results

1) Electricity Price Volatility

The electricity prices from the two scenarios over the 24-hour horizon are depicted in Fig. 7 (a), (b), respectively. Moreover, different DR participation levels are considered, which include 10% DR (10% of the customers are involved in the DR programs), 20% DR and 30% DR cases. The impact of the different- level DR on the electricity price is shown in Fig.7.b.

As we can see in Fig. 7(a), the electricity prices in S1 fluctuate widely, especially in weekdays when the electricity demand waves more sharply.

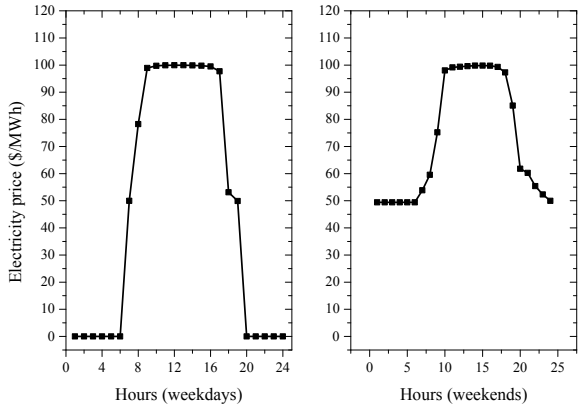

Fig. 7(a). Electricity prices in S1.

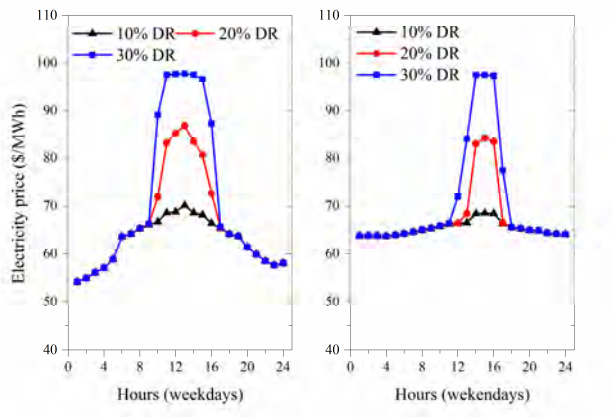

Fig. 7(b). Electricity prices in S2.

Compared with the electricity price shown in Fig. 7. (a), we can see that the DR programs contribute to reducing the volatility electricity price. With the consideration of 10% DR, the electricity price fluctuation range is narrowed down to 54-98$/MWh in weekdays and 63-98$/MWh in weekends. When the DR participation level increases to 30%, the electricity price fluctuation range is further narrowed down to 54-70$/MWh in weekdays and 63-69$/MWh in weekends, which indicates that a lower volatility of the electricity price can be achieved in S2. Moreover, it can be seen that the time of peak electricity price can be reduced by the DR, and the effect can be more obvious with higher DR participation level. This is mainly due to the response of aggregators' energy demand with the electricity price. Such response of the aggregator is shown in Fig.8. When the electricity is oversupplied due to the increased electricity production from the wind power, the electricity price can be relatively low and aggregator therefore may increases the electric heating ($L^t_{es,i}$). Then, the aggregated demand for electricity increases while the aggregated demand for heat decreases. Therefore, CHP units can decrease the amount of heat and electricity produced. The increased electricity demand along with the decreased electricity production from CHP units raises the electricity price. During the peak-hours, on the contrary, the decreased electricity demand together with the increased production of CHP units reduces the electricity price.

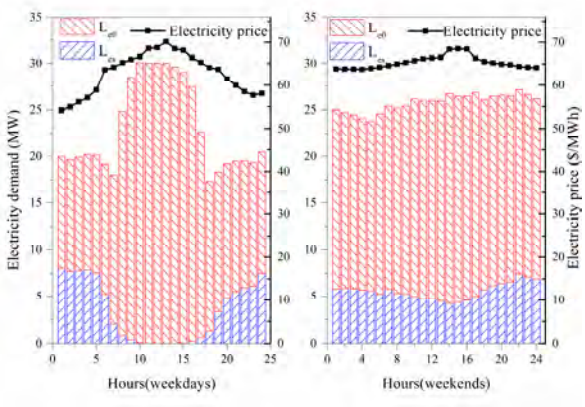

Fig. 8. Aggregators' response with the electricity price.

2) Wind Power Accommodation

For covering both the lower wind power output scenario and higher wind power output scenario, two cases are considered. The capacity of the wind farms is set as 47MW to model the 5% wind power penetration level in case 1, and the capacity of the farms are set as 100MW to model the 10% wind power penetration level in case 2.

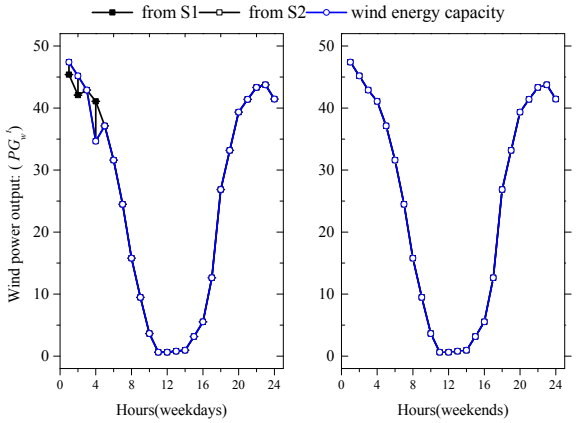

Fig. 9. (a). Wind power output in S1 and S2: 5% wind power.

This article has been accepted for publication in a future issue of this journal, but has not been fully edited. Content may change prior to final publication. Citation information: DOI 10.1109/TSTE.2017.2731786, IEEE Transactions on Sustainable Energy

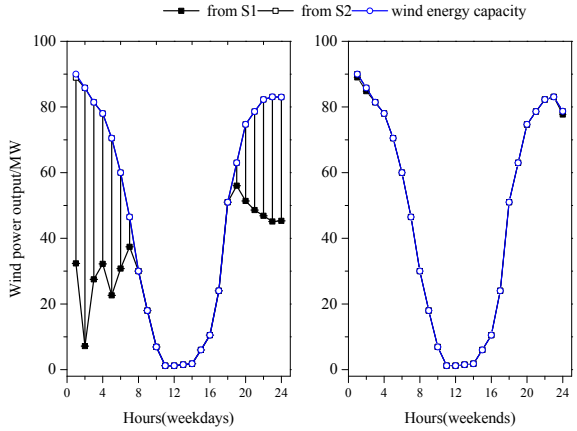

Fig. 9.b. Wind power output in S1 and S2: 10% wind power.

The simulation results in terms of wind power accommodation are shown in Fig. 9. One observation from the results is that the wind power curtailment only occurs during off-peak hours in weekdays in 5% wind power case. To meet the customers' pre-determined and constant heat demand, CHP units have to remain on and generate a certain amount of electricity, which occupies part of the proportion of wind power generation. Since the wind power output in 5% wind power case is relatively low, there is no need of curtailment in most of the time. The other observation is that a severe curtailment happens when the wind power penetration level increases to 10% in S1. Moreover, in S2, the wind power curtailment can be mitigated remarkably. During the off-peak hours, the relatively low electricity price makes customers shift the heat demand to electric heating, leading to the decrease in the electricity production from CHP units and increase in electricity demand. Thereby, the wind power output can be fully utilized.

3) Social Welfare

The social welfare results in S1 and S2 are compared and shown in Table III.

TABLE III
SOCIAL WELFARE ($/h)

Scenarios		Weekdays	Weekends
S1		5207	6031
S2	10% DR	5612	6223
	20% DR	5853	6356
	30% DR	6069	6435

From Table III, we can see that the social welfare in S2 is much higher than that in S1. With the consideration of 10% DR, the social welfare in S2 increases by 405$/h and 192$/h in weekdays and weekends, respectively. In other word, the social welfare in weekdays increases by 7.8% and the social welfare in weekends increases by 3.2% if 10% of the customers participate in the DR programs. If 30% of the customers are involved in the DR program, the social welfare in weekdays further increases by 16.6% while the social welfare in weekends further increases by 6.7%. Moreover, given that the electricity demand fluctuates more drastically in weekdays than in weekends, we can draw the conclusion that the customers' flexible resources could be more valuable when there is a high volatility of electricity demand. The total social welfare increase is calculated as 753,627 $ per year with the consideration of 10% DR, assuming that only winter is taken into account. When the DR level increases to 20% and 30%, the total social welfare increases will further increase to 1,213,885$ and 1,601,202$, respectively. The increase of the social welfare gives reasons to encourage the DR programs and offsets the investment cost of such DR programs.

VI. CONCLUSIONS

The inharmony between the variable wind power and the wide use of combined heat and power (CHP) has become a significant barrier to the efficient utilization of the wind power. A lot of researches have been conducted on increasing the flexibility of CHP based energy system, from the production and the network sides. This paper investigates the utilization of the customers' flexible energy demand to provide additional balancing resources and release the inharmony between the variable wind power and the wide use of CHP. We find that the integration of heat and electricity systems provides multiple options to customers for fulfilling their energy demand. The built-in flexibility in customers' energy demand provides desirable flexible resources for maintaining the balance between energy supply and demand and achieving the efficient utilization of the wind power.

REFERENCES

[1] B. Zeng, J. Zhang, X. Yang, J. Wang, J. Dong, and Y. Zhang, "Integrated Planning for Transition to Low-Carbon Distribution System With Renewable Energy Generation and Demand Response," *IEEE Transactions on Power Systems,* vol. 29, pp. 1153-1165, 2014.

[2] G. Streckienė, V. Martinaitis, A. N. Andersen, and J. Katz, "Feasibility of CHP-plants with thermal stores in the German spot market," *Applied Energy,* vol. 86, pp. 2308-2316, 2009.

[3] P. F. Bach, "Towards 50% wind electricity in Denmark: Dilemmas and challenges," *European Physical Journal Plus,* vol. 131, pp. 1-12, 2016.

[4] X. Lu, M. B. McElroy, W. Peng, S. Liu, C. P. Nielsen, and H. Wang, "Challenges faced by China compared with the US in developing wind power," *Nature Energy,* vol. 1, p. 16061, 05/23/online 2016.

[5] M. G. Nielsen, J. M. Morales, M. Zugno, T. E. Pedersen, and H. Madsen, "Economic valuation of heat pumps and electric boilers in the Danish energy system," *Applied Energy,* vol. 167, pp. 189-200, 2015.

[6] T. Jónsson, P. Pinson, and H. Madsen, "On the market impact of wind energy forecasts," *Energy Economics,* vol. 32, pp. 313-320, 2010.

[7] X. Chen, C. Kang, M. O. Malley, Q. Xia, J. Bai, C. Liu, *et al.*, "Increasing the Flexibility of Combined Heat and Power for Wind Power Integration in China: Modeling and Implications," *IEEE Transactions on Power Systems,* vol. 30, pp. 1848-1857, 2015.

[8] A. Fragaki and A. N. Andersen, "Conditions for aggregation of CHP plants in the UK electricity market and exploration of plant size," *Applied Energy,* vol. 88, pp. 3930-3940, 2011.

[9] Z. Li, W. Wu, J. Wang, B. Zhang, and T. Zheng, "Transmission-Constrained Unit Commitment Considering Combined Electricity and District Heating Networks," *IEEE Transactions on Sustainable Energy,* vol. 7, pp. 480-492, 2016.

[10] J. Duquette, A. Rowe, P. Wild, and J. Yan, "Thermal performance of a steady state physical pipe model for simulating district heating grids with variable flow," *Applied Energy,* vol. 178, pp. 383-393, 2016.

[11] X. Zhang, M. Shahidehpour, A. Alabdulwahab, and A. Abusorrah, "Optimal Expansion Planning of Energy Hub With Multiple Energy Infrastructures," *IEEE Transactions on Smart Grid,* vol. 6, pp. 2302-2311, 2015.

[12] M. Moeini-Aghtaie, P. Dehghanian, M. Fotuhi-Firuzabad, and A. Abbaspour, "Multiagent Genetic Algorithm: An Online Probabilistic View on Economic Dispatch of Energy Hubs Constrained by Wind Availability," *IEEE Transactions on Sustainable Energy,* vol. 5, pp. 699-708, 2014.

[13] J. Sjödin and D. Henning, "Calculating the marginal costs of a district-heating utility," *Applied Energy,* vol. 78, pp. 1-18, 2004.

[14] S. Bahrami and A. Sheikhi, "From Demand Response in Smart Grid Toward Integrated Demand Response in Smart Energy Hub," *IEEE Transactions on Smart Grid,* vol. 7, pp. 650-658, 2016.

[15] A. Sheikhi, M. Rayati, S. Bahrami, and A. M. Ranjbar, "Integrated Demand Side Management Game in Smart Energy Hubs," *IEEE Transactions on Smart Grid,* vol. 6, pp. 675-683, 2015.

[16] P. Mancarella and G. Chicco, "Real-Time Demand Response From Energy Shifting in Distributed Multi-Generation," *Smart Grid IEEE Transactions on,* vol. 4, pp. 1928-1938, 2013.

[17] Pirouti and Marouf, "Modelling and analysis of a district heating network," *Cardiff University,* 2013.

[18] J. Gustafsson, J. Delsing, and J. V. Deventer, "Improved district heating substation efficiency with a new control strategy," *Applied Energy,* vol. 87, pp. 1996-2004, 2010.

[19] J. Duquette, A. Rowe, and P. Wild, "Thermal performance of a steady state physical pipe model for simulating district heating grids with variable flow," *Applied Energy,* vol. 178, pp. 383-393, 2016.

[20] X. S. Jiang, Z. X. Jing, Y. Z. Li, Q. H. Wu, and W. H. Tang, "Modelling and operation optimization of an integrated energy based direct district water-heating system," *Energy,* vol. 64, pp. 375-388, 2013.

[21] B. Rolfsman, "Combined heat-and-power plants and district heating in a deregulated electricity market," *Applied Energy,* vol. 78, pp. 37-52, 2004.

[22] C. Ruiz and A. J. Conejo, "Pool Strategy of a Producer With Endogenous Formation of Locational Marginal Prices," *Power Systems IEEE Transactions on,* vol. 24, pp. 1855-1866, 2009.

[23] W. Yu-Chi, A. S. Debs, and R. E. Marsten, "A direct nonlinear predictor-corrector primal-dual interior point algorithm for optimal power flows," *IEEE Transactions on Power Systems,* vol. 9, pp. 876-883, 1994.

[24] J. D. Weber and T. J. Overbye, "A two-level optimization problem for analysis of market bidding strategies," in *Power Engineering Society Summer Meeting*, 1999, pp. 682-687 vol.2.

[25] H. Wang, C. E. Murillo-Sánchez, R. D. Zimmerman, and R. J. Thomas, "On Computational Issues of Market-Based Optimal Power Flow," *IEEE Transactions on Power Systems,* vol. 22, pp. 1185-1193, 2007.

[26] C. Wang and M. H. Nehrir, "Analytical approaches for optimal placement of distributed generation sources in power systems," *IEEE Transactions on Power Systems,* vol. 19, pp. 2068-2076, 2004.

[27] L. Pedersen, "Method for Load Modelling of Heat and Electricity Demand," 10th International Symposium on District Heating and Cooling, 3-5 September 2006, p.4.

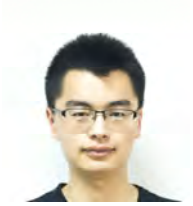

Changzheng Shao (S'17) received the B.S. degree in electric engineering from Shandong University. He is currently pursuing the Ph.D. degree in electric engineering from Zhejiang University, Hangzhou, China.

His research interests include operation and optimization of the integrated energy system, and the power market.

Yi Ding (M'10) received the bachelor's and Ph.D. degrees in electrical engineering from Shanghai Jiaotong University, Shanghai, China, and Nanyang Technological University, Singapore in 2002 and 2007, respectively.

He is a Professor with the College of Electrical Engineering, Zhejiang University, Hangzhou, China. His current research interests include power systems reliability/performance analysis incorporating renewable energy resources, smart grid performance analysis, and engineering systems reliability modeling and optimization.

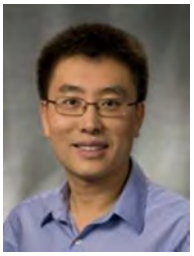

Jianhui Wang (SM'12) received the Ph.D. degree in electrical engineering from Illinois Institute of Technology, Chicago, Illinois, USA, in 2007.

Presently, he is an Associate Professor with the Department of Electrical Engineering at Southern Methodist University, Dallas, Texas, USA. He also holds a joint appointment as Section Lead for Advanced Power Grid Modeling at the Energy Systems Division at Argonne National Laboratory, Argonne, Illinois, USA.

Dr. Wang is the secretary of the IEEE Power & Energy Society (PES) Power System Operations, Planning & Economics Committee. He is an associate editor of Journal of Energy Engineering and an editorial board member of Applied Energy. He has held visiting positions in Europe, Australia and Hong Kong including a VELUX Visiting Professorship at the Technical University of Denmark (DTU). Dr. Wang is the Editor-in-Chief of the IEEE Transactions on Smart Grid and an IEEE PES Distinguished Lecturer. He is also the recipient of the IEEE PES Power System Operation Committee Prize Paper Award in 2015.

Yonghua Song (F'08) received the B.E. and Ph.D. degrees from the Chengdu University of Science and Technology, Chengdu, China, and the China Electric Power Research Institute, Beijing, China, in 1984 and 1989, respectively, all in electrical engineering.

From 1989 to 1991, he was a Postdoctoral Fellow at Tsinghua University, Beijing, China. He then held various positions at Bristol University, Bristol, U.K.; Bath University, Bath, U.K.; and John Moores University, Liverpool, U.K., from 1991 to 1996. In 1997, he was a Professor of Power Systems at Brunel University, where he was a Pro-Vice Chancellor for Graduate Studies since 2004. In 2007, he took up a Pro-Vice Chancellorship and Professorship of Electrical Engineering at the University of Liverpool, Liverpool. He was a Professor at the Department of Electrical Engineering, Tsinghua University, where he was an Assistant President and the Deputy Director of the Laboratory of Low-Carbon Energy in 2009. In 2012, he became the Executive Vice-President of Zhejiang University. His current research interests include smart grid, electricity economics, and operation and control of power systems.

Prof. Song was the recipient of the D.Sc. Award by Brunel University, in 2002, for his original achievements in power system research. He was elected as the Vice-President of Chinese Society for Electrical Engineering (CSEE) and appointed as the Chairman of the International Affairs Committee of the CSEE in 2009. In 2004, he was elected as a Fellow of the Royal Academy of Engineering, U.K.